21st Annual Conference of the Canadian Nuclear Society
Toronto, Ontario, Canada / June 11-14, 2000

The origin of anisotropy DHC behavior in Zr-2.5%Nb pressure tube materials

SungSoo Kim*, Sang Chul Kwon, Kee Nam Choo,
YongMoo Cheong, and Young Suk Kim
Korea Atomic Energy Research Institute,
P. O. Box 105, Yousung-Ku, Taejon 305-353, Korea

Abstract

In order to explain the anisotropy of delayed hydride cracking (DHC) behavior in the longitudinal and in radial direction in Zr-2.5%Nb pressure tube materials, DHC tests using compact tension (CT) and cantilever beam (CB) specimens and tensile tests using small specimens with a gage length of about 2 mm have been carried out, and the texture change in the DHC surfaces have been examined. It has been found that the deformation mechanisms operating during the cracking process were significantly different in both specimens. The $(10\bar{1}2)$ twinning system operated when a DHC crack propagated in the longitudinal direction and both the $(11\bar{2}1)$ and $(10\bar{1}2)$ twinning systems operated when the DHC crack propagated in the radial direction. The tensile results showed that there is anisotropy of the tensile behavior and the strength in the radial direction is minimum in the range of 100-400°C. This behavior seems to be due to the anisotropy of texture.

Therefore, it can be concluded that the differences in crack propagation behavior between CT and CB specimens is due to the differences in deformation mechanisms which are resulted from the anisotropy of the texture.

1. Introduction

It is reported that there is anisotropic DHC behavior in the longitudinal and radial direction in curved compact tension (CCT) and cantilever beam (CB) specimen, respectively [1, 2]. The crack growth rate in the longitudinal direction is two times faster than that of the radial direction and the threshold stress intensity factor for DHC (K_{IH}) initiation in the longitudinal direction is smaller by about 50% than that of the radial direction in the compact tension (CT) and cantilever beam (CB) specimen, as shown in Fig. 1 [1] and Fig. 2 [2-7]. Although the cracking planes and the basal pole components are identical in both specimens, except for the crack growth directions being different in both specimens, there is anisotropic DHC behavior. This suggests that there is an effect of crack growth direction on anisotropic DHC behavior in pressure tube materials.

The effect of texture on K_{IH} has been investigated using a Zr-2.5%Nb plate and this effect has been explained properly by the rule of mixture using the basal pole component (F) in the loading direction as the volume fraction of a brittle hydride and the rest of it (1-F) as the volume fraction of a ductile matrix [3]. Although the explanation may be different, a similar suggestion has been provided by Coleman et al. [8].

There has been no systematic investigation to identify the origin of anisotropic DHC behavior, and therefore, the cracking surface and tensile properties are examined and analyzed in this study.

2. Experimental

DHC tests were performed using CT and CB specimens with 60ppm hydrogen, as shown in Fig. 3. The CT specimens were tested using a constant load creep tester. The CB specimens were tested using a computer-controlled tester, which used acoustic emissions (AE) to detect cracking. Both cracking planes were examined by XRD to determine the texture change after cracking due to DHC. The change in texture during DHC was confirmed and the change in the basal pole components was calculated. The normalized inverse pole figures are constructed again to show the change in texture and the deformation mechanism operated clearly.

The strength and deformation behavior in the radial, longitudinal, and transverse direction were investigated using small tensile specimen with a gage length about 2 mm long, as shown in Fig. 4. The specimens were machined by electro deposit machining (EDM) and the EDM surface of about 0.1 mm was removed by grinding. The tensile tests were carried out in the range of RT to 560°C and the strain rate was $5x10^{-4}$/s. The displacement was used as strain during the tensile test.

3. Results and Discussion

The texture of a CANDU pressure tube is shown in Fig. 5, using inverse pole figures. The basal plane normals of the zirconium crystals are aligned in the transverse direction, and the prism plane normals are aligned in the longitudinal direction. These pole figures show how grain orientations are changed along the radial and longitudinal direction in CB and CT specimens during cracking.

The basal pole components at the fracture surfaces were decreased by about 10% and 20% after cracking in the radial and longitudinal direction, respectively, as shown in Fig. 6 and 7. This shows that there has been certain plastic deformation during cracking, even due to DHC.

It has been found that the deformation mechanisms operating during the cracking process were different in both directions, as shown in Fig. 6 c) and 7 c). The $(10\bar{1}2)$ twinning system operated when the DHC crack propagated in the longitudinal direction in the CT specimens, and both the $(11\bar{2}1)$ and $(10\bar{1}2)$ twinning systems operated when the DHC crack propagated in the radial direction in the CB specimens. These phenomena can be explained using Fig. 5. If the DHC process proceeds under the plane strain condition and there is plastic deformation during DHC, then the plastic strain may be existed only in the transverse and longitudinal direction in the CT specimens, and in the transverse and the radial direction in the CB specimens. Therefore, only the $(10\bar{1}2)$ twinning system can operate in the CT specimens, referring to Fig. 5 b) and c), while both the $(11\bar{2}1)$ and $(10\bar{1}2)$ twinning systems can operate in the CB specimens, referring to Fig. 5 a) and b).

The yield and tensile strength are compared together in Fig. 8 and 9, respectively. The yield strength in the radial direction is lowest in the range of 100-400°C, whereas the tensile strength is lowest in the entire range of the test.

The stress-strain curves at about 170-250°C in the radial, longitudinal, and transverse direction are shown in Fig. 10. The work hardening behavior in the radial direction is different from those of the longitudinal and transverse direction, and the total elongation in the radial direction is minimum. These differences may be due to the anisotropy of the texture, as explained above.

These observations may be summarized as follows: 1) there is certain plastic deformation in the DHC surface, 2) the operating deformation mechanisms are different in the radial and longitudinal direction in the CB and CT specimens, respectively, 3) the strength and work hardening behavior are different. All of these seem to be due to the anisotropy of texture, and may change the DHC behavior.

The anisotropy of the deformation behavior may cause a different plastic behavior during DHC. The grain orientations vary significantly along the radial direction, compared to along the longitudinal and transverse direction. This grain distribution in the radial direction may allow relatively isotropic deformation behavior. Therefore, the resistance to DHC may be increased in the radial direction. It can be concluded that the difference in crack propagation behavior between the CT and the CB specimens is due to a difference in the grain orientation and the deformation mechanisms in the cracking direction, which result from the difference in texture.

Therefore, in order to interpret and predict the DHC crack growth behavior, the strength, work hardening behavior and texture in the crack propagation direction should be considered in addition to the strength in the loading direction and the basal pole component in the cracking plane.

4. Conclusions

1) The origin of the anisotropy of the DHC behavior according to the cracking direction is the anisotropy of the texture and deformation mechanisms operating during the DHC process.

2) Only the $(10\bar{1}2)$ twinning system operated when the DHC crack propagated in the longitudinal direction and both the $(11\bar{2}1)$ and $(10\bar{1}2)$ twinning system operated when the DHC crack propagated in the radial direction.

3) The strength, work hardening behavior and texture in the crack propagation direction should be considered to properly interpret and predict the DHC behavior, in addition to the strength in the loading direction and the basal pole component in the cracking plane.

Acknowledgements

This work has been carried out in the CANDU Pressure Tube Materials project as a part of the Nuclear R&D program funded by the Ministry of Science and Technology in Korea.

References

1. S. Sagat, C. E. Coleman, M. Griffiths, and B. J. S. Wilkins, Zirconium in the Nuclear Industry, Tenth International Symposium, ASTM STP 1245, 1994, pp. 35-61.

2. S. S. Kim, S. C. Kwon, K. N. Choo, Y. M. Cheong, and Y. S. Kim, Key Engineering Materials, to be published.

3. S. S. Kim, S. C. Kwon, and Y. S. Kim, J. Nucl. Mater. Vol. 273, 1999, pp.52-59.

4. C. E. Coleman, S. Sagat, and K. F. Amouzouvi, Control of Microstructure to Increase the Tolerance of Zirconium Alloys to Hydride Cracking, Atomic Energy of Canada Limited Report AECL-9524 (1987).

5. C. E. Coleman, Zirconium in the Nuclear Industry, Fifth Conference, ASTM STP 754, 1982, pp. 393-411.

6. H. Huang, and W. J. Mills, Metal. Transactions A, 22A (1991), pp.2149-2060.

7. W. J. Mills, and F. H. Huang, Eng. Frac. Mech. 39 (1991), pp. 241-257.

8. C. E. Coleman, B. A. Cheadle, C. D. Cann, and J. R. Theaker, Zirconium in the Nuclear Industry, Eleventh International Symposium, ASTM STP 1295, 1996, pp. 884-898.

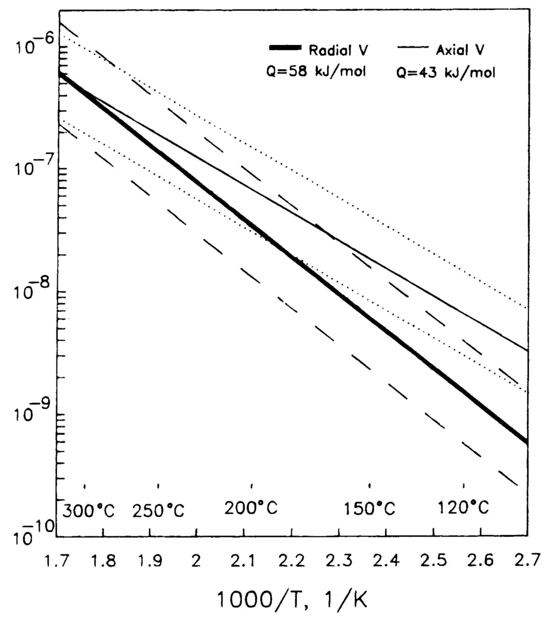

Fig. 1. Comparison of DHC velocity in the radial and longitudinal direction [1].

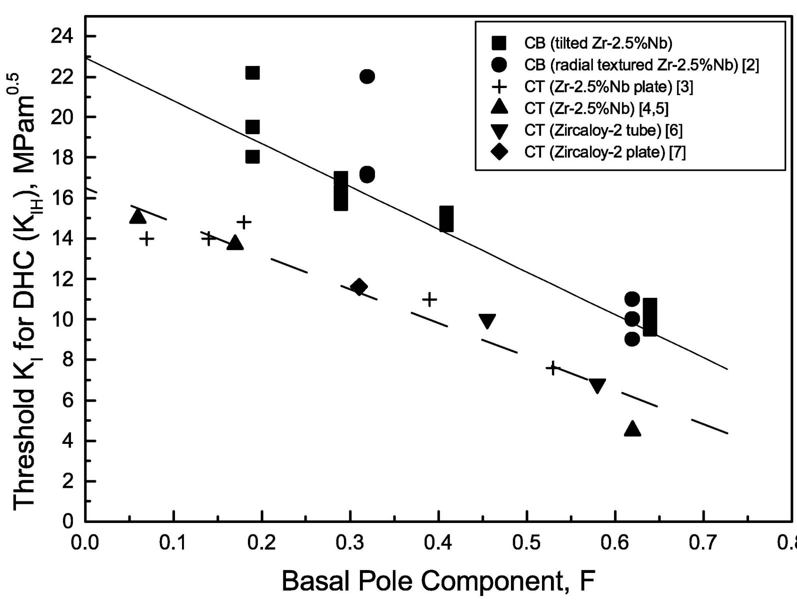

Fig. 2. Comparisons of K_{IH} measured from CT and CB specimens with the basal pole components in Zircaloy-2 and Zr-2.5%Nb materials [2-7].

a) cantilever beam specimen b) curved compact tension specimen

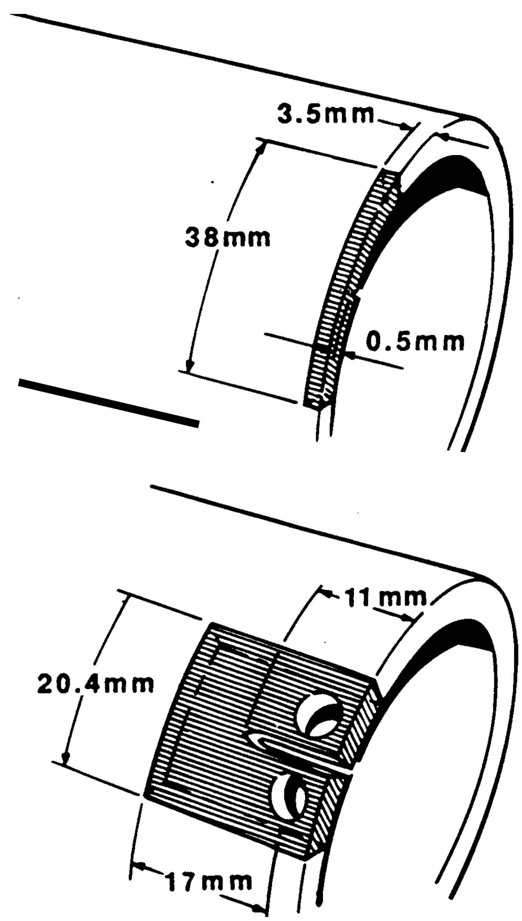

Fig. 3. Schematic illustration of a) cantilever beam (CB) and b) curved compact tension (CCT) specimens [1].

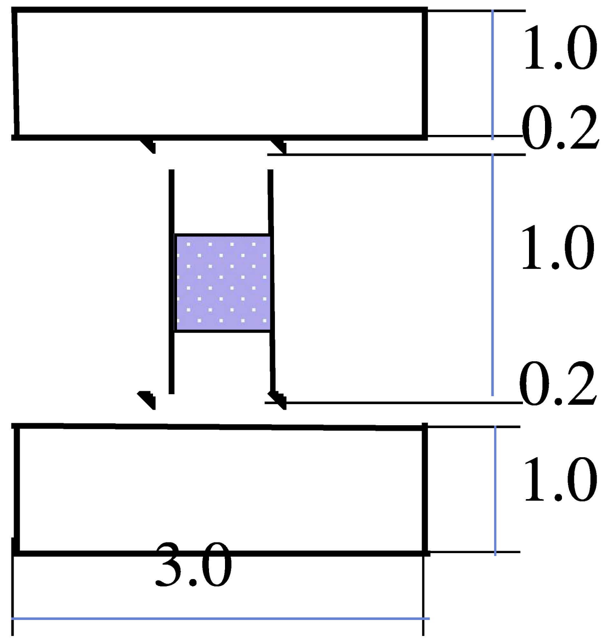

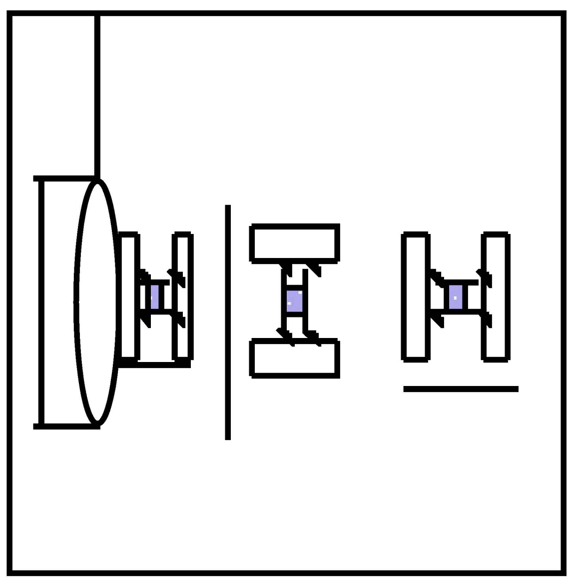

Fig. 4. The geometry of a small tensile specimen and a diagram of the machining in a pressure tube.

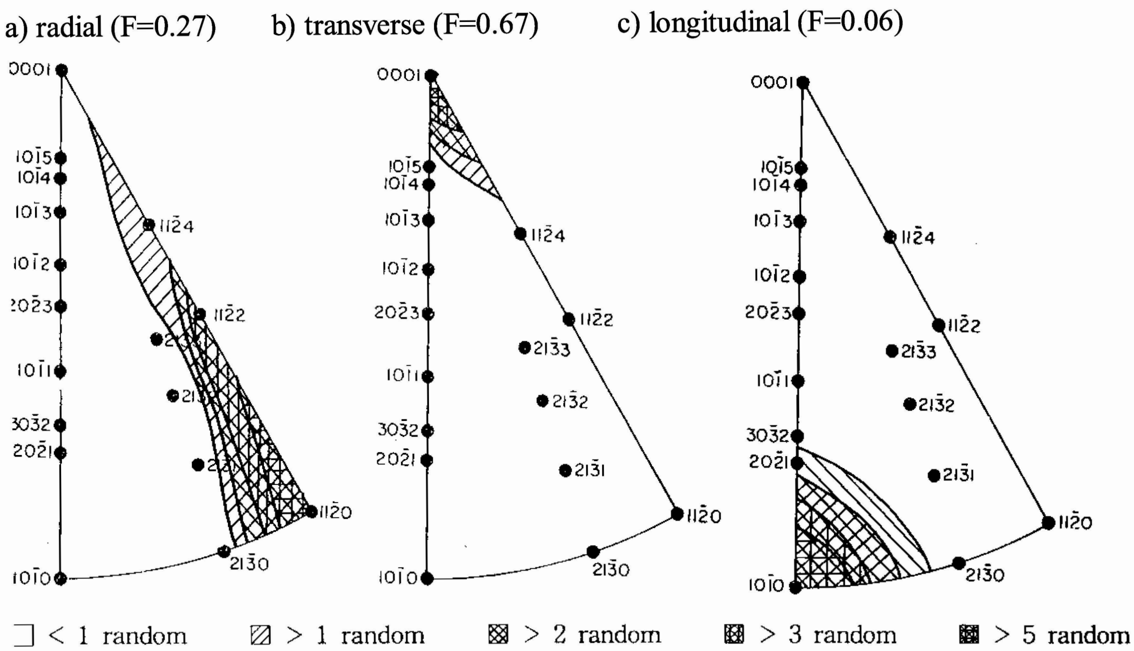

Fig. 5. Inverse pole figures for as-received Zr-2.5%Nb pressure tube material.

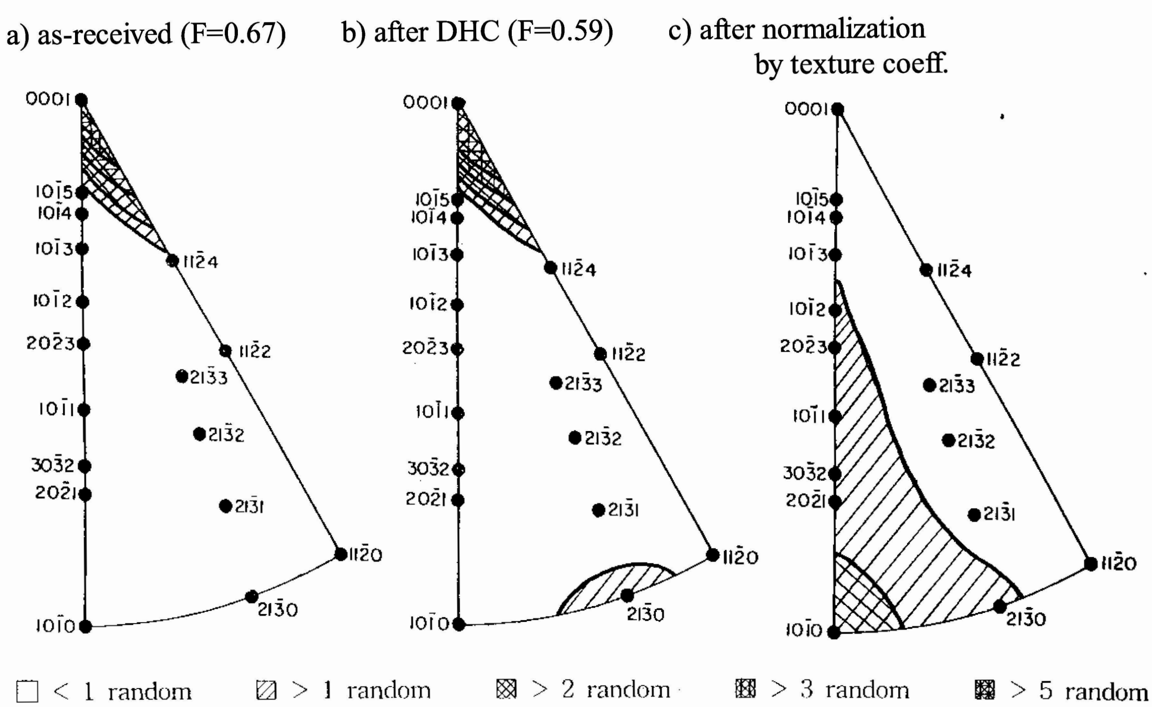

Fig. 6. Comparison of texture before and after cracking in the radial direction.

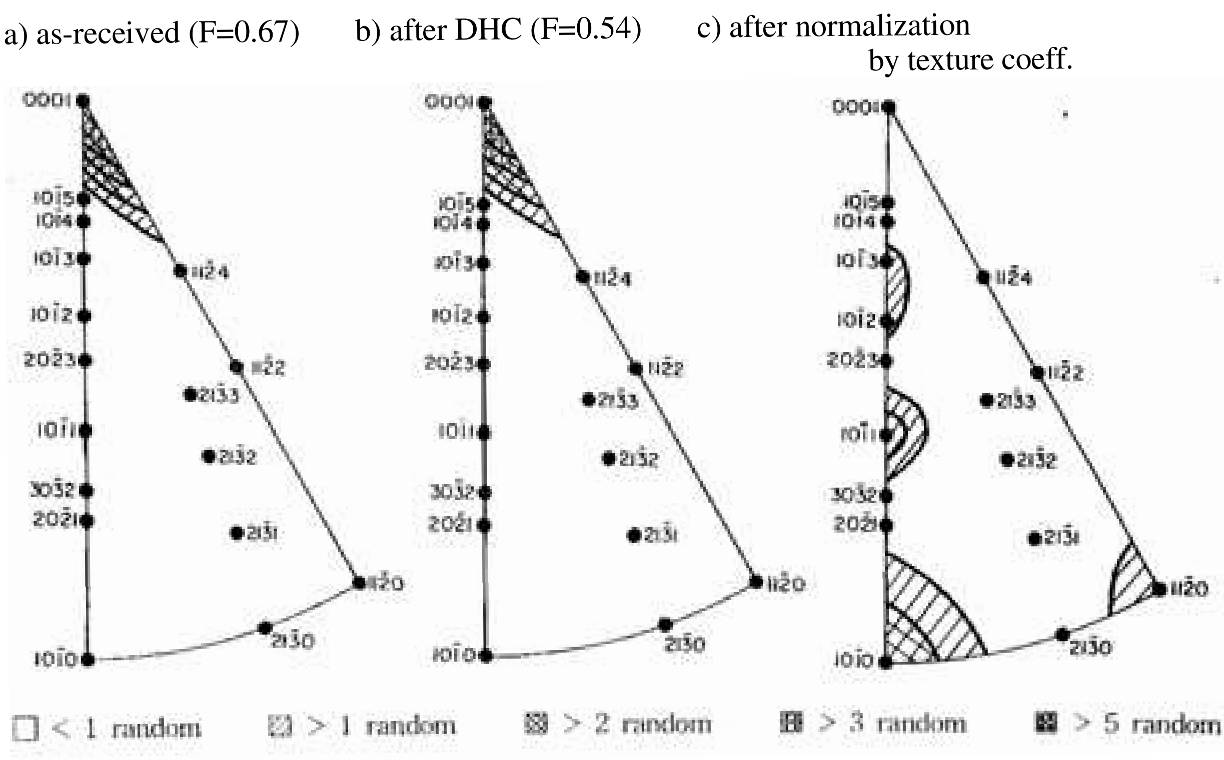

Fig. 7. Comparison of textures before and after cracking in the longitudinal direction.

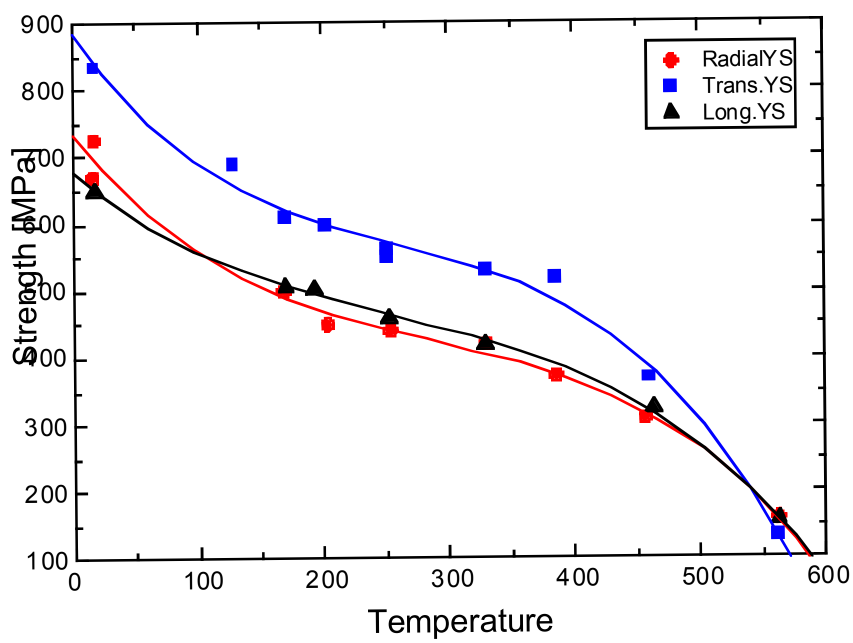

Fig. 8. Comparison of the yield strength in the radial, longitudinal, and transverse direction.

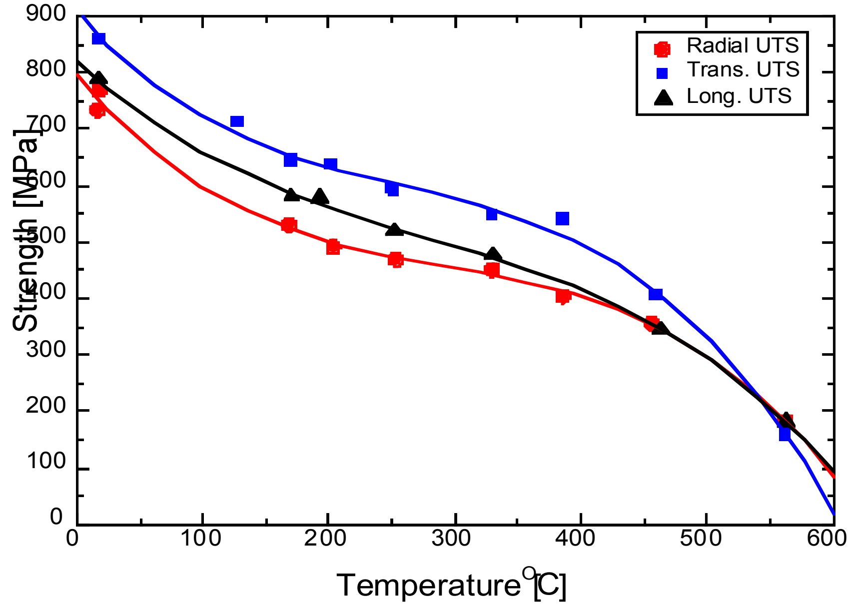

Fig. 9. Comparison of the tensile strength in the radial, longitudinal, and transverse direction.

a) longitudinal direction

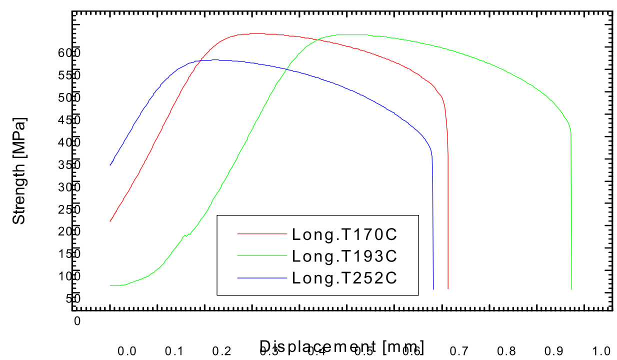

b) radial direction

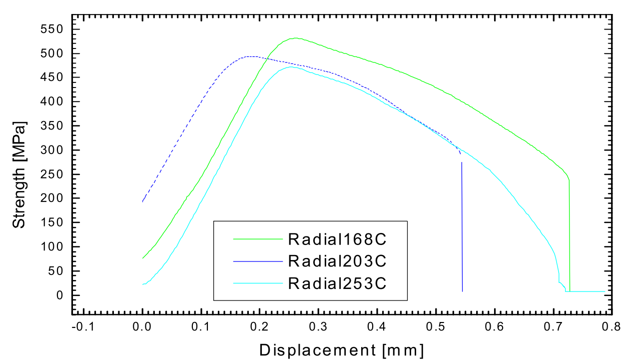

c) transverse direction

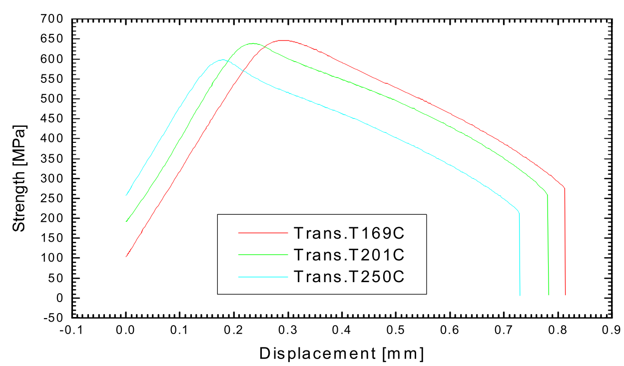

Fig. 10. Comparison of stress-strain curves for radial, transverse, and longitudinal direction in Zr-2.5%Nb pressure tube materials at room temperature.